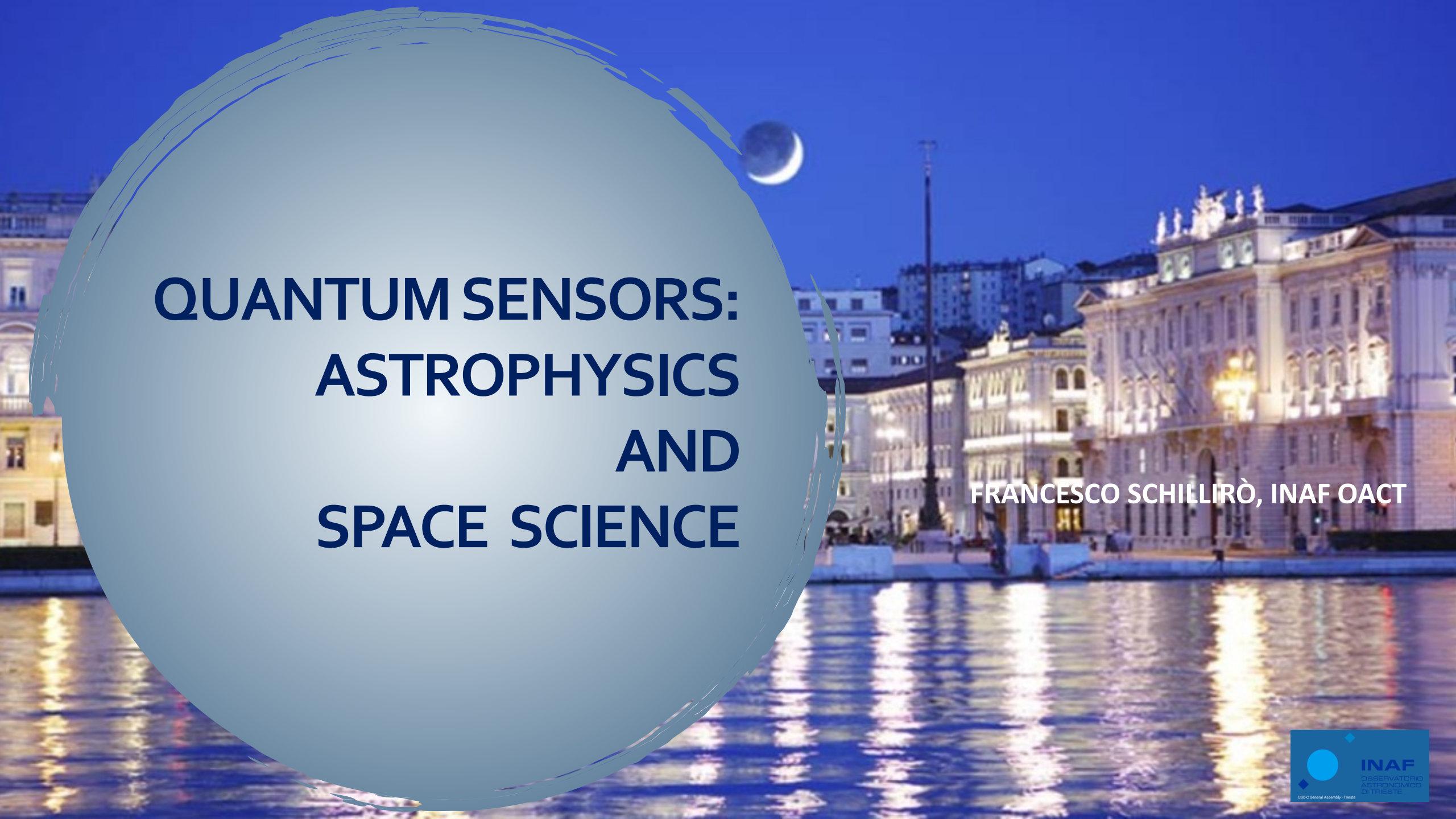

QUANTUM SENSORS: ASTROPHYSICS AND SPACE SCIENCE

FRANCESCO SCHILLIRÒ, INAF OACT

INAF
OSSERVATORIO ASTRONOMICO DI TRIESTE
USC-C General Assembly - Trieste

WHAT IS QUANTUM SENSING

Quantum sensing includes all measurement techniques that exploit quantum states of matter or light to detect physical and chemical quantities with precision beyond classical limits.

Quantum sensors offer sensitivity that surpasses the limits of classical physics. They can detect extremely weak signals and measure quantities with very high precision, operating at the level of quantum noise.

Quantum sensing protocols can be broadly divided into two classes, depending on how the measurement affects the quantum state:

Quantum Sensing Measurement Strategies

Projective Measurements:

- Measurement **collapses the quantum state** (wavefunction collapse)
- Information obtained in a **single strong readout**
- The system must be **re-prepared after each measurement**

Widely used in **qubit-based quantum sensors**

Examples

Single-photon detectors perform a **strong projective measurement** of the photon-number state. $|\psi\rangle=\alpha|0\rangle+\beta|1\rangle$ Measurement projects the state onto $|0\rangle$ or $|1\rangle$ and the photon is **irreversibly absorbed by the detector**.

Prepare → Evolve → Projective Measure → Reset

Quantum Sensing Measurement Strategies

Non-demolition (weak) Measurements

- Measurement extracts information while **minimally disturbing the quantum state**
- Enables **repeated interrogation** of the same quantum system
- **Preserves quantum coherence** over longer times
- Reduces measurement back-action
- Can help surpass the **Standard Quantum Limit**

Examples
Dispersive measurements
NV-center sensing protocols

Prepare → Evolve → QND → Evolve → QND

Quantum Sensing Strategies

A very effective solution is:

combining the two

RAMSEY PROTOCOL

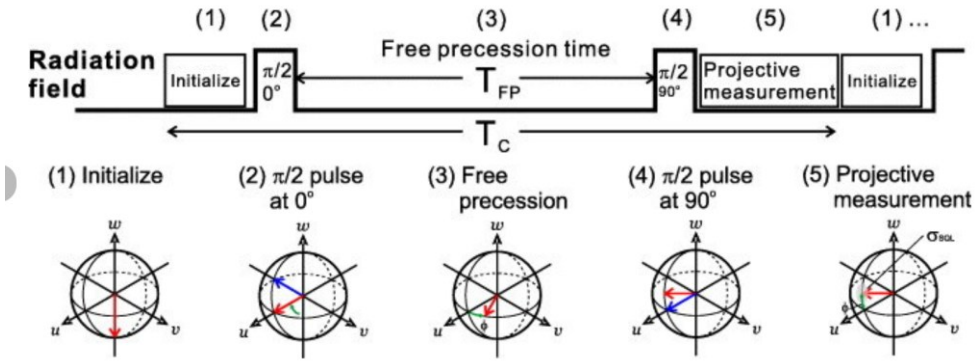

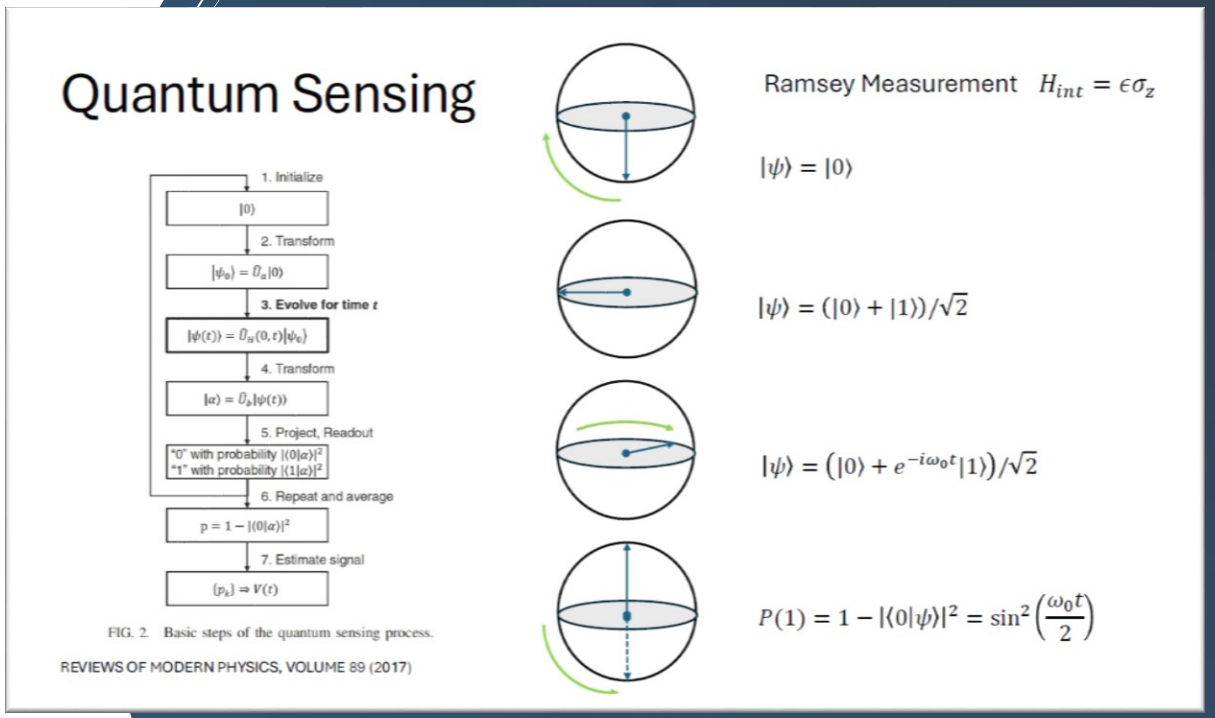

$$T \lesssim T_2^*$$

$$\delta B \propto \frac{1}{\gamma\sqrt{NT}}$$

The free evolution time in a Ramsey protocol is chosen experimentally and is typically limited by the coherence time T_2^* of the quantum sensor.

T_1 (relaxation time) is the characteristic time over which a quantum system exchanges energy with its environment and relaxes from an excited state to its ground state. It describes **energy relaxation** and the recovery of thermal equilibrium.

T_2 (dephasing time) is the timescale over which the relative phase between quantum states is lost due to interactions with the environment or noise. It characterizes the **loss of quantum coherence**, even when no energy relaxation occurs.

T_2^* (effective dephasing time) describes the **decay of the transverse component of the Bloch vector** due to loss of phase coherence, caused by environmental noise and inhomogeneities that make different spins accumulate different phases over time.

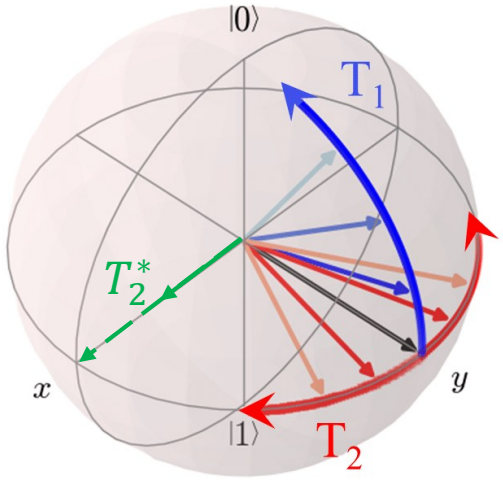

Two examples of QND Sensing

$$T \lesssim T_2^* \qquad \delta B \propto \frac{1}{\gamma\sqrt{NT}}$$

Superconductive Qbit in cavity resonator

Diamonds NV Centers

Axions and Dark Matter Detection

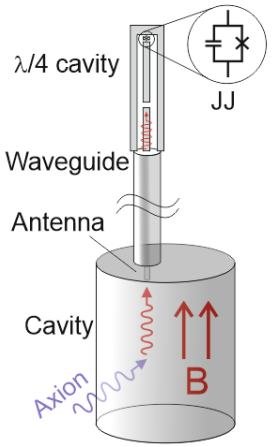

Axion: is a light, extremely weakly interacting particle that could constitute dark matter and can be experimentally searched for through its conversion into photons in a strong magnetic field.

Axions Detector

The principle of operation of a haloscope is shown in Fig. 1: an axion couples to the strong magnetic field (10 T) converting into a microwave (5-10 GHz) photon (an excitation of a cavity mode) inside the cavity; a superconducting (SC) device (JJ in figure 1) is coupled to the cavity mode either

$$\nu \simeq \frac{m_a c^2}{h} \qquad m_a \sim 1\ \mu eV - 100\ \mu eV$$

The photon frequency is set by the axion mass and is essentially independent of the applied magnetic field, which only controls the conversion probability.

$$P_a \propto g_{a\gamma\gamma}^2 B_0^2 V Q \rho_a$$

haloscope

$$P_a \sim 10^{-23} - 10^{-24}\ \mathrm{W}$$

1 μeV → 240 MHz

10 μeV → 2.4 GHz

100 μeV → 24 GHz

Axions and Dark Matter Detection

$$P_a \sim 10^{-23} - 10^{-24}\ \mathrm{W}$$

$$E_\gamma = h\nu \sim 6.6 \times 10^{-24}\ \mathrm{J}$$

$$\dot{N} = \frac{P_a}{h\nu}$$

$$\dot{N} \sim 0.1 - 1\ \text{fotoni/s}$$

The expected axion conversion rate is of the order of one photon per second or even lower, which means we are operating in an ultra-rare single-photon regime.

Fundamental Limit of Linear Microwave Amplifiers

A phase-insensitive linear amplifier is fundamentally limited by the **Standard Quantum Limit (SQL)**.

It must add at least:

$$n_{add} \geq \frac{1}{2}$$

half a photon of noise per mode.

This is a **quantum mechanical constraint**, not a technological limitation.

Equivalent Noise Count Rate

At frequency $\nu \sim 10\,\mathrm{GHz}$:

$$E_\gamma = h\nu \approx 6.6 \times 10^{-24}\ \mathrm{J}$$

The equivalent photon noise rate in a detection bandwidth $\Delta\nu$ is:

$$\dot{N}_{noise} \sim n_{add}\,\Delta\nu$$

For a typical bandwidth of:

$$\Delta\nu \sim 1\,\mathrm{MHz}$$

$$\dot{N}_{noise} \sim 0.5 \times 10^{6}$$

$$\boxed{\dot{N}_{noise} \sim 5 \times 10^{5}\ \text{photons/s}}$$

A phase-insensitive microwave amplifier adds at least half a photon of noise per mode, corresponding to an equivalent noise rate of hundreds of kHz in a MHz bandwidth — 5 orders of magnitude larger than the expected axion signal rate.

Superconductive Qubit in cavity resonator

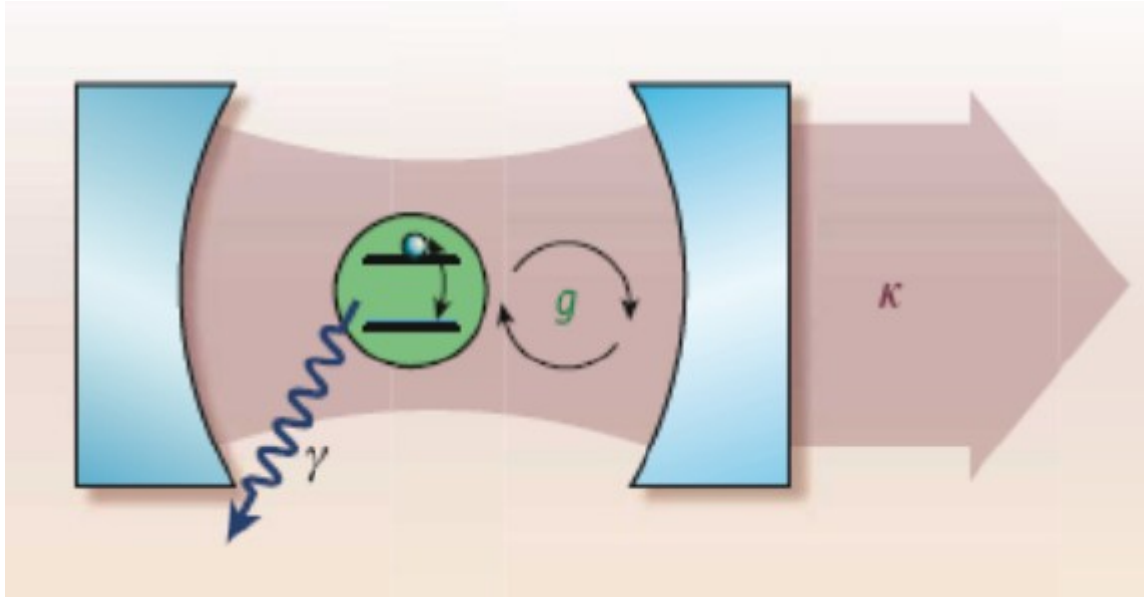

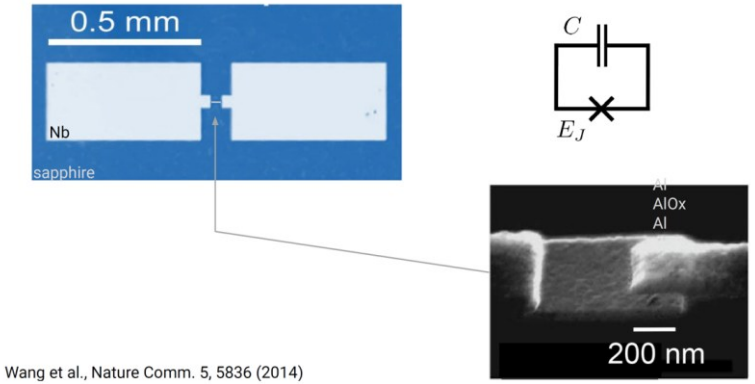

Wang et al., Nature Comm. 5, 5836 (2014)

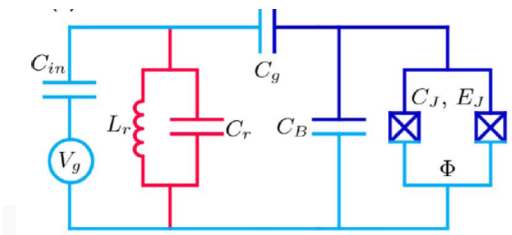

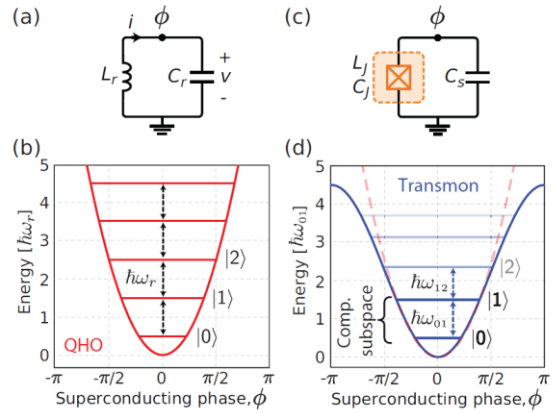

A **transmon** is a type of **superconducting qubit** based on a Josephson junction shunted by a large capacitor, designed to reduce sensitivity to charge noise. It is widely used in quantum computing because it provides **improved coherence times and stable qubit control**.

Nonlinear inductance= anharmonic oscillator

Superconductive Qbit in cavity resonator

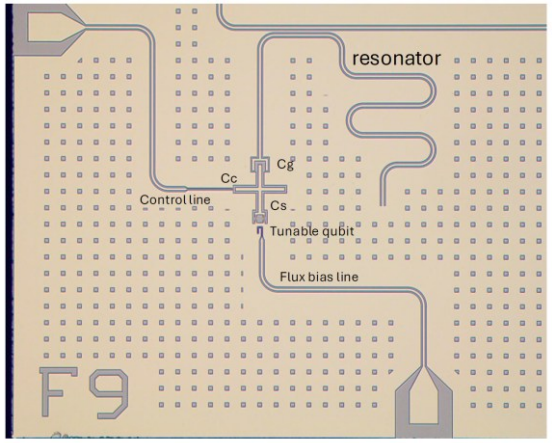

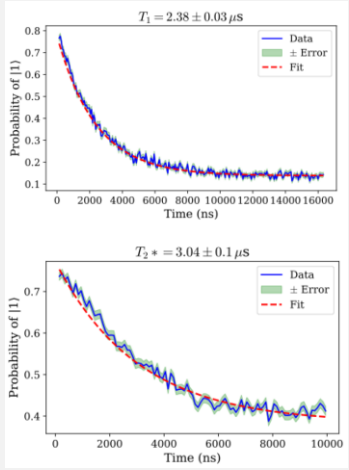

2D Resonator Transmon

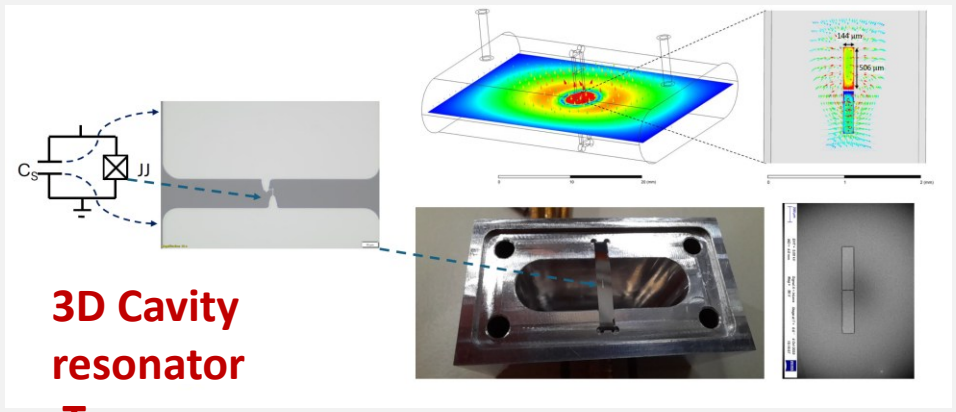

3D Cavity resonator Transmon

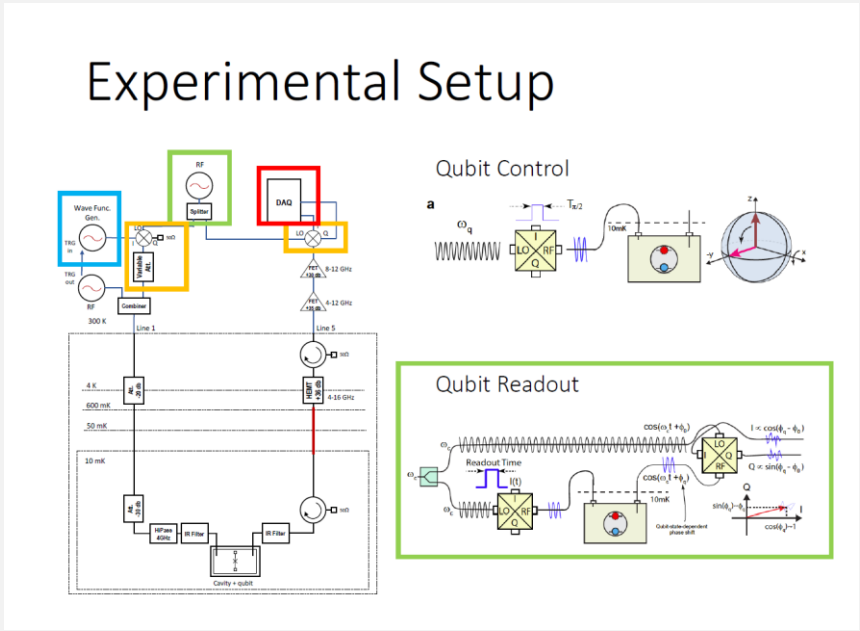

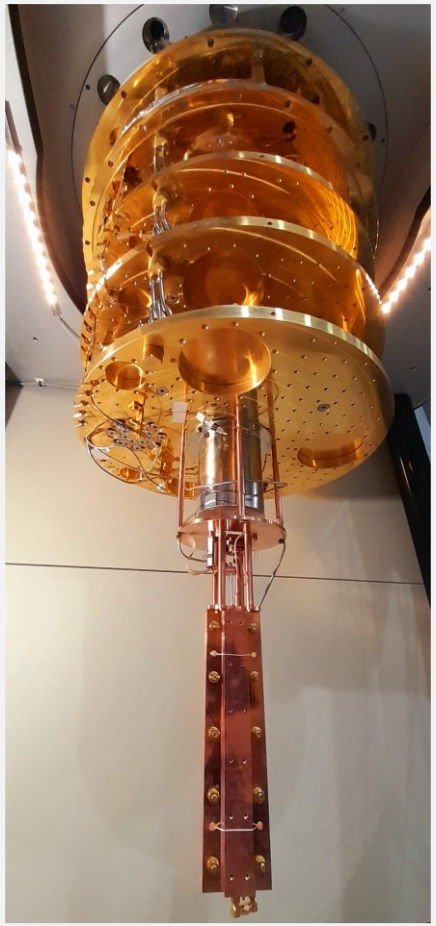

Superconductive Qubit in cavity resonator

Quantum Non-Demolition (QND) Measurement

A measurement is QND if the measured observable $\hat{O}$ satisfies:

$$[\hat{O}, \hat{H}] = 0$$

For photon detection in a cavity:

$$\hat{O} = a^\dagger a$$

where:

- $a, a^\dagger$ = annihilation and creation operators of the **cavity photon mode**
- $a^\dagger a$ = photon-number operator

QND implies:

- Photon number is preserved
- No photon absorption
- Repeated measurements possible

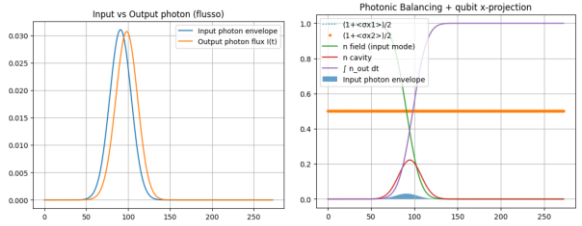

Figure 3.1: Summary of the photonic and qubit dynamics during the protocol. Left: input vs. output photon envelope. Right: photon balancing (field and cavity occupations) and qubit X-projection. The transient intracavity population enables dispersive phase accumulation on the qubits.

Qubit–Photon Interaction in the Dispersive Regime

In circuit QED, a superconducting qubit interacts with a **single cavity mode**:

$$H_{JC} = \omega_c a^\dagger a + \frac{\omega_q}{2}\sigma_z + g(a\sigma_+ + a^\dagger \sigma_-)$$

- a = cavity photon
- $\sigma_\pm$ = qubit excitation operators
- g = qubit–photon coupling strength

If the qubit and cavity are strongly detuned:

$$|\Delta| = |\omega_q - \omega_c| \gg g$$

No real energy exchange occurs.

Effective Dispersive Hamiltonian

Applying a second-order Schrieffer–Wolff transformation:

$$H_{\text{eff}} \simeq (\omega_c + \chi\sigma_z)\, a^\dagger a + \frac{1}{2}(\omega_q + \chi)\,\sigma_z$$

with

$$\chi = \frac{g^2}{\Delta}$$

Superconductive multi-Qubit and Entangled Multi Qubit sensor

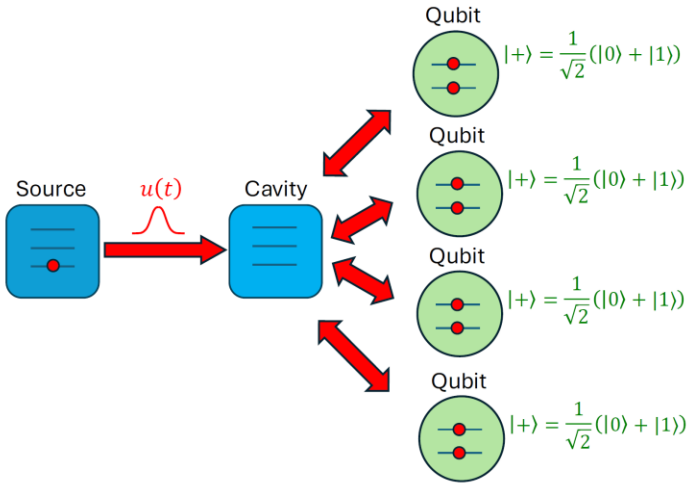

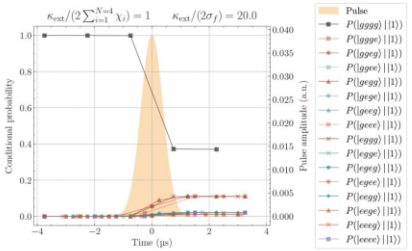

Sensing with Multiqubit Entangled States

Greenberger–Horne–Zeilinger (GHZ) state

$$|\psi\rangle = (|000000\ldots\rangle + |111111\ldots\rangle)/\sqrt{2}$$

$$|\psi\rangle = \left(|000000\ldots\rangle + e^{-iN\omega_0 t}|1111111\ \ldots\rangle\right)/\sqrt{2}$$

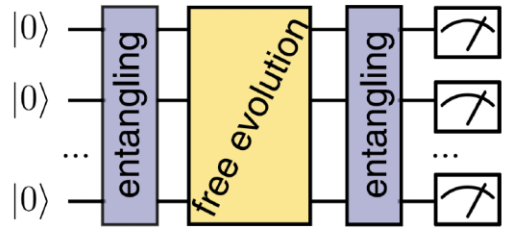

$$P = 1 - |\langle 0|\psi\rangle|^2 = \sin^2\left(N\frac{\omega_0 t}{2}\right)$$

Scaling Sensitivity as $\frac{1}{\sqrt{N}}$

Scaling Sensitivity as $\frac{1}{N}$

To go beyond the quantum limit of linear amplification, it has to replace amplitude measurement with phase-based QND photon-number detection

Diamonds NV Centers

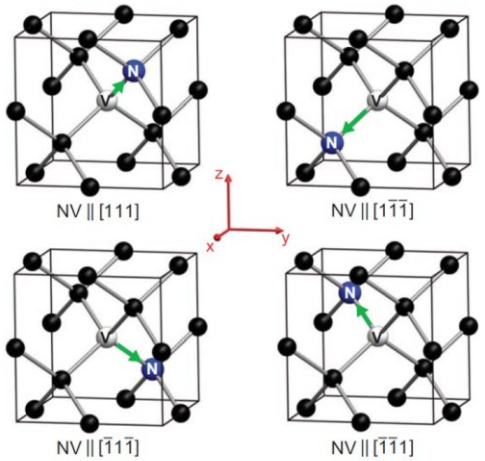

Diamond Lettice doped with nitrogen atoms and Carbon Vacancies

Osservable measured is the total Spin along the defect direction;

S=0 -> singlet state with m_s=0
S=1-> triplet state with m_s=-1,0,1

In the ground state of the NV^- center, the total spin is S = 1 (triplet), giving three spin sublevels $m_s = 0, \pm 1$.

Due to the crystal-field anisotropy along the N–V axis, the $m_s = 0$ and **$m_s = \pm 1$** states have different energies.

Zero-Field Splitting is about 2.87 GHz.

Ground state

- $^3A_2$ — ground triplet state

Excited state

- ^3E — excited triplet state

Metastable states

- $^1A_1$ — metastable singlet state
- ^1E — metastable singlet state

637 nm fluo

532 nm laser

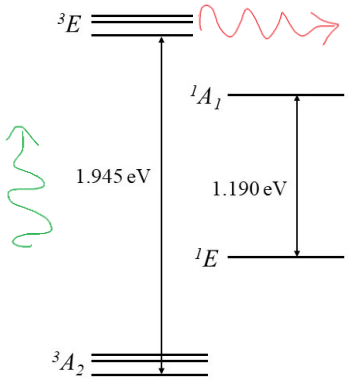

Less fluo for metastable states
InterSystem Crossing

ZFS and Zeeman Effect

In the ground state of the NV^- center, the total spin is S = 1 (triplet), giving three spin sublevels $m_s = 0, \pm 1$.

Due to the crystal-field anisotropy along the N–V axis, the $m_s = 0$ and $m_s = \pm 1$ states have different energies.
Zero-Field Splitting is about 2.87 GHz.

$$H_{\mathrm{ZFS}} = D\,\hat{S}_z^2 \qquad D \approx 2.87\ \mathrm{GHz}.$$

The spin has a **magnetic moment**. If a magnetic field **B** is applied, an **interaction energy (Zeeman energy)** appears that depends on how much the spin is **projected along the field direction**.
In the formalism, this corresponds to the term

$$H_Z = \gamma_e \mathbf{B} \cdot \hat{\mathbf{S}}$$

which is the **electron Zeeman term** in the NV Hamiltonian.
If we choose the z-axis along the NV axis and apply a magnetic field B|| along the defect axis, the Hamiltonian simplifies to

$$H \simeq D\hat{S}_z^2 + \gamma_e B_{\parallel} \hat{S}_z$$

ZFS and Zeeman Effect

- **At $B = 0$:** a single resonance appears at ~2.87 GHz (the transitions $m_s = 0 \leftrightarrow m_s = \pm 1$ overlap).
- **For $B \neq 0$:** two resonances appear, one for $m_s = 0 \leftrightarrow +1$ and one for $m_s = 0 \leftrightarrow -1$.

$$H \simeq D\hat{S}_z^2 + \gamma_e B_{\parallel} \hat{S}_z$$

The frequencies (standard approximation, magnetic field aligned with the NV axis) become

$$f_{\pm} \approx D \pm \gamma_e B_{\parallel}$$

and the separation between the two peaks is

$$\Delta f = f_+ - f_- \approx 2\gamma_e B_{\parallel}$$

with

$$\gamma_e = g\mu_B/h \approx 2.8\ \mathrm{MHz/G}.$$

Key point for sensing: what matters is the **projection of the magnetic field along the NV axis**, $B_{\parallel}$.

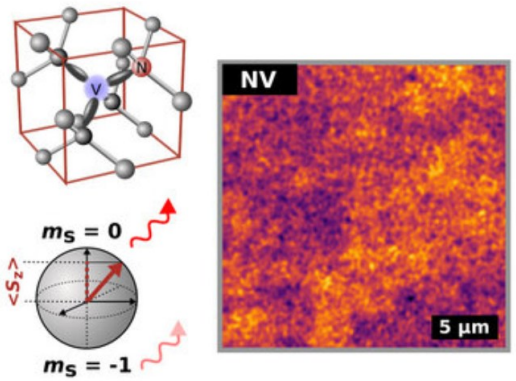

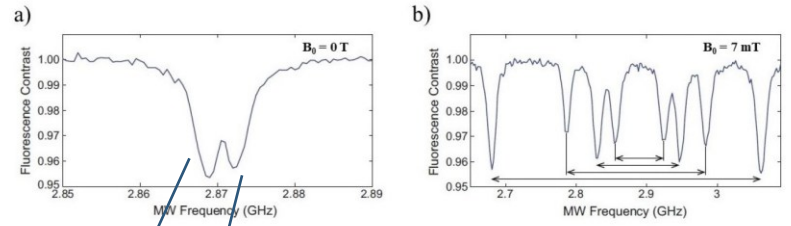

Figure 1.8: a) ESR spectrum at zero applied static magnetic field. The small splitting is induced by local non-axial strain at the NV center. b) ESR spectrum with an applied static magnetic field of ~7 mT. The field is applied along arbitrary direction, resulting in a different field projection on each of the four possible NV symmetry axes and thus four pairs of transitions. [6]

fluo dip

States $m_s = \pm 1$ are more susceptible to decade for metastable states

CW-ODMR Protocol

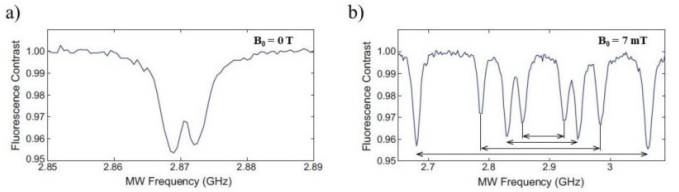

Figure 1.8: a) ESR spectrum at zero applied static magnetic field. The small splitting is induced by local non-axial strain at the NV center. b) ESR spectrum with an applied static magnetic field of ∼7 mT. The field is applied along arbitrary direction, resulting in a different field projection on each of the four possible NV symmetry axes and thus four pairs of transitions. [6]

Continuous-Wave Optically Detected Magnetic Resonance

Principle

In the **CW-ODMR protocol**, the magnetic field is measured by observing the **shift of spin resonance frequencies**, which appear as **fluorescence dips** due to the higher probability of **intersystem crossing (ISC)** when the spin is in the $m_s = \pm 1$ states.

Experimental sequence

- **Laser ON** → optically polarizes the NV center into $m_s = 0$
- **Microwave frequency sweep** → scans possible spin resonances
- **Microwave at resonance** → induces transition $m_s = 0 \leftrightarrow m_s = \pm 1$
- **ISC becomes more probable** → reduced fluorescence
- **Observed signal** → **fluorescence dip**
- **Dip position** → **magnetic field**

Without microwaves

- Continuous optical excitation
- Optical pumping polarizes the system into $m_s = 0$
- The NV center emits **high fluorescence**

Reference state: high fluorescence

Microwaves off resonance

- No spin transitions are induced
- Spin remains in $m_s = 0$
- Optical cycle remains in the **bright state**

Fluorescence remains unchanged

Microwaves at resonance

When the MW frequency satisfies

$$f = D \pm \gamma B_{\parallel}$$

- transition $m_s = 0 \leftrightarrow m_s = \pm 1$ is induced
- part of the population moves to $m_s = \pm 1$

These states:

- more frequently enter **intersystem crossing (ISC)**
- spend time in **metastable singlet states (dark)**
- emit **fewer photons**

➡ **Total fluorescence decreases (ODMR dip)**

Role of the magnetic field

The magnetic field:

- **shifts the resonance frequencies**
- **lifts the degeneracy between $m_s = +1$ and $m_s = -1$**

Therefore:

- $B = 0$ → **one dip at 2.87 GHz**
- $B \neq 0$ → **two dips separated by**

$$\Delta f = 2\gamma B_{\parallel}$$

Measuring the **shift of the dips** allows the **magnetic field to be determined**.

Quantum Sensors in Astrophysics

Quantum sensors enable extremely precise measurements of weak physical signals, opening new possibilities in astrophysical observations.

Main applications

Magnetic field measurements

- Mapping magnetic fields in the interstellar medium
- Studying magnetospheres of planets and stars
- Investigating magnetic turbulence in astrophysical plasmas

Dark matter searches

- Detection of ultralight dark matter candidates
- Axion-like particle searches using spin precession experiments
- Precision magnetometry for exotic field detection

Gravitational wave detection

- Quantum-enhanced interferometry
- Use of squeezed states to surpass the standard quantum limit
- Improved sensitivity in detectors such as LIGO and Virgo

Precision spectroscopy in astronomy

- Ultra-stable atomic clocks for astronomical spectroscopy
- Improved calibration of telescopes and spectrographs

Fundamental physics tests

- Tests of Lorentz invariance
- Search for variations of fundamental constants
- Tests of general relativity with ultra-precise clocks

Quantum Sensors for Space and Navigation

Quantum sensing technologies are promising tools for next-generation space missions and autonomous navigation systems.

Main applications

Quantum magnetometry in space missions

- Measurement of planetary magnetic fields
- Monitoring solar wind and space plasma
- CubeSat-based magnetic field mapping

Quantum gravimetry and accelerometry

- High-precision inertial sensors for spacecraft navigation
- Gravity field mapping of planets and moons
- Detection of subsurface structures

Quantum clocks for navigation

- Ultra-precise atomic clocks for deep-space navigation
- Improved satellite positioning systems
- Next-generation GNSS technologies

Quantum inertial navigation

- Atom interferometer gyroscopes and accelerometers
- Navigation without GPS signals
- Autonomous navigation for spacecraft and planetary rovers

Space-based quantum experiments

- Tests of quantum mechanics in microgravity
- Space-based atom interferometers
- Long-baseline quantum communication experiments

THANKS

Francesco Schillirò

+39 0957332210

francesco.schilliro@inaf.it

www.oact.inaf.it

INAF OSSERVATORIO ASTRONOMICO DI TRIESTE

USC-C General Assembly - Trieste